

Transverse galvanomagnetic and thermomagnetic coefficients of a molybdenum single crystal*

R. Fletcher

Physics Department, Queen's University, Kingston, Canada

(Received 9 June 1976)

With the magnetic field aligned along [100] and the current along [110], the following transport coefficients have been determined: the transverse and Hall electrical resistivities, the transverse and Righi-Leduc thermal resistivities, and the Nernst-Ettingshausen coefficient. If the transverse electrical resistivity is represented as B^n (B is the magnetic field), then n is found to peak at about 1.90 as B increases, and steadily decline at higher fields. The lattice thermal conductivity is extracted from the data by two methods, the results of which are not identical but are within experimental uncertainty. The Nernst-Ettingshausen coefficient yields a density of electronic states consistent with that derived from specific-heat work, in agreement with recent theoretical predictions.

I. INTRODUCTION

In comparison with the electrical properties, the thermal properties of metals in high magnetic fields have received relatively little attention. This is partly due to the increased difficulties involved in measuring the latter, and partly because the galvanomagnetic properties have usually been investigated with a view to obtaining the topological properties of the Fermi surface, and the thermomagnetic properties are not expected to yield significantly different information in this context. However, if one wishes to calculate the detailed properties in the regime where electrons are scattered by phonons, it should be somewhat easier to begin with the thermal coefficients, since the angle through which an electron is scattered is not of primary importance, in contrast to the case of the electrical coefficients.

Some recent experimental results also suggest that more effort in this general area can be rewarding. Thus a simultaneous measurement of the lattice thermal conductivity of tungsten,¹ utilizing both the transverse thermal resistivity and the Righi-Leduc thermal resistivity yielded two different results; this discrepancy may result from the large deviation from equilibrium of the electronic distribution that can occur in compensated metals under the influence of high magnetic fields. A study of the thermomagnetic properties of Cd, another compensated metal, has been useful² as a comparison with the galvanomagnetic properties; in particular, the detailed form of the behavior of the thermal resistivity in comparison with the electrical resistivity indicated that it would probably be more profitable to attempt a calculation of these quantities using a real Fermi surface rather than look for explanations in terms of intersheet scattering of the electrons.

The present investigation on molybdenum was begun with these previous experiments in mind. Both the transverse and Hall electrical resistivities, as well as the transverse and Righi-Leduc thermal resistivities, have been determined on the same sample. A useful aspect about dealing with compensated metals is that it is much easier to experimentally determine the Nernst-Ettingshausen coefficient as compared with the case of uncompensated metals. The significance of this coefficient was examined in a previous paper,³ where it was shown that it should yield a direct measure of the density of states of the electrons at the Fermi level without the complication of electron-phonon enhancement. Since Ref. 3 was published, it has been shown⁴ that thermoelectric coefficients are indeed enhanced by the electron-phonon interaction so that specific-heat and transport data should both yield the same result. We have measured the Nernst-Ettingshausen coefficient of Mo during the present experiments; the high Debye temperature should ensure that the electronic scattering is almost purely elastic at the temperatures of interest here.

II. EXPERIMENTAL METHODS

The Mo single crystal⁵ was spark machined to a shape similar to that described previously.² A flat plate of dimensions $35 \times 6.5 \times 0.9$ mm was first produced by wire cutting, and large portions of this were cut away, leaving thin transverse limbs. The final width of the sample was about 3 mm, and the length between the longitudinal limbs (those used for the measurement of the transverse electrical and thermal resistivities) was about 16 mm. The long axis, i.e., the current direction, was aligned along [110] to within 1° , and the normal to the plate (the field direction) was along [100] to

within 0.5° . The sample was mounted in the cryostat using a conducting cement made from silver powder (obtained by allowing silver paint to settle and decanting off the excess liquid) and plastic cement.⁶ This provides a strong bond which can be repeatably cycled to helium temperatures. The direction of the magnetic field was arranged to be normal to the sample surface to an accuracy of 0.25° .

The experimental techniques have been outlined elsewhere,² and only improvements will be mentioned here. The calibration of the carbon thermometers and the method of obtaining temperature differences was the same as previously used, with the exception that the use of the derivative of the resistance with temperature to obtain the temperature differences was replaced by an absolute determination of the two temperatures involved. This gives an identical accuracy at small temperature differences, but is an improvement at relatively large ones, say 0.2 K at 4.2 K, since it eliminates the errors due to higher derivatives. The temperature was stabilized by a feedback regulator which monitors the helium vapor pressure using a capacitance gauge, and regulates the pumping speed by means of a solenoid valve. This provides a control independent of magnetic field and is capable of 1 mK or better at any temperature.

The initial data showed the sample has a rather low residual resistance ratio (r) of $1690 \pm 3\%$ (this is $R_{293}/R_{4.2}$). The sample was removed and cleaned of all mounting cement using acetone, followed by a solution made up of equal volumes of HCl and H_2O_2 . It was then heated to 1800°C for 2 h with an initial vacuum of 10^{-5} Torr, which increased to about 5×10^{-5} Torr during the heating. This treatment improved r to $5050 \pm 5\%$. It was later discovered that this treatment was almost the optimum that could have been used to reduce the carbon content to low levels.⁷ According to this previous work, the final impurities are probably mainly tungsten. The sample was again tested for alignment by x-ray diffraction, and subsequently remounted in the same manner as before. We shall refer to the unannealed and annealed sample as $1u$ and $1a$, respectively.

III. RESULTS AND DISCUSSION

A. General considerations

We shall use a notation consistent with that of Grenier *et al.*⁸ (conveniently summarized by Long⁹), who define various adiabatic and isothermal tensors. Assuming the magnetic field \vec{B} to be along z and the current along x , we have determined the isothermal electrical transverse and Hall resistivities ρ_{11} and ρ_{21} defined according to

$$\begin{aligned}\rho_{11} &= \frac{1}{2} [\rho_{xx}(\vec{B}) + \rho_{xx}(-\vec{B})], \\ \rho_{21} &= \frac{1}{2} [\rho_{yx}(\vec{B}) - \rho_{yx}(-\vec{B})].\end{aligned}$$

We find ρ_{xx} to be independent of the direction of \vec{B} (i.e., $\pm z$) to within the experimental uncertainty. ρ_{21} is evaluated by suitable reversals of the current and field to eliminate any component of ρ_{11} due to slight misalignment of the transverse limbs; with \vec{B} along a high-symmetry axis we do not anticipate any transverse even components of ρ_{21} , but the data treatment would eliminate these in any event. An examination of the original results that any transverse even components must be less than about 15% of the magnitude of ρ_{21} at any field and temperature. The adiabatic thermal transverse and Righi-Leduc resistivities γ_{11}^m and γ_{21}^m were determined in a similar manner, except, of course, that the thermal current was not reversed. We use the superscript m to denote the measured quantities for reasons which become clear in the discussion. Again γ_{11}^m was independent of field direction. Finally we have measured the adiabatic Nernst-Ettingshausen coefficient ϵ_{21} [defined as $-E_y/(\partial T/\partial x)$, and given the symbol Q^a in a previous publication³]. We have not investigated the thermoelectric component ϵ_{11} in this work.

It is always useful to have estimates of the quantity $\omega_c\tau$, where ω_c is the cyclotron frequency and τ is the relaxation time. Using the measured electronic specific heat and the estimated area of the Fermi surface, Loucks¹⁰ estimated $\langle 1/v \rangle^{-1} \sim 7.6 \times 10^5 \text{ m sec}^{-1}$, where v is the local electronic velocity. Assuming $\langle v \rangle \sim \langle 1/v \rangle^{-1}$ (which is probably reasonably accurate since the measured cyclotron masses and dimensions are all reasonably consistent with this velocity), and using the measured Fermi surface area¹¹ of 24 \AA^{-2} , together with the room-temperature resistivity¹² of $5.3 \mu\Omega \text{ cm}$ enables the average room-temperature relaxation time τ to be estimated as $\sim 1.6 \times 10^{-14} \text{ sec}$. For \vec{B} along [001], the highest cyclotron mass will be obtained for the external orbit of the large electron surface¹⁰ at Γ (the jack), and will be $\sim 2.7m$, where m is the electron mass. At 4.2 K, for sample $1u$, this yields $\omega_c\tau \sim 1.7B$ (B in tesla) for sample $1a$, $\omega_c\tau \sim 5.3B$. Although relatively complete data on the anisotropy of the electronic lifetime exists for some of the surfaces in Mo,¹³ there are as yet no results for the jack surface, so the effect of anisotropy on the estimated $\omega_c\tau$ is not known. It is, however, encouraging that the other surfaces exhibit a relatively isotropic orbital lifetime for a variety of impurities. The data was taken up to fields of 3.8–5.2 T (two different solenoids of different upper limits were used) so that sample $1a$ should be well into the high-field region at the upper fields, but sample $1u$ is somewhat marginal.

All other orbits have much lower cyclotron masses, giving correspondingly higher values of $\omega_c\tau$.

B. Transverse resistivities ρ_{11} and γ_{11}^m

The Debye temperature¹⁴ of Mo is 474 K so that by 4.2 K, both samples are well into the residual resistance regime. Any change in resistivity at zero field on cooling from 4.2 to 1.3 K is below the experimental uncertainties, but at high fields it is easily measured and amounts to an increase of about 1.9% for sample 1*a*, and about 0.5% for sample 1*u*. Figure 1 shows the variation of $\rho_{11}(B) - \rho_{11}(0)$, with B at 4.2 K in the form of a Kohler plot. The zero-field resistivity $\rho_{11}(0)$ is a small correction for both samples and, except at the very lowest fields, Fig. 1 is essentially a graph of $\rho_{11}(B)$. The relative uncertainties in ρ_{11} are of the order of 0.1% for each sample, and 1% for comparisons between samples. (Sample 1*a* was slightly reduced in dimensions by the cleaning solution so the form factors are slightly different.) The major uncertainties in the absolute values plotted in Fig. 1 arise from r which is known to $\pm 5\%$ for sample 1*a*, and $\pm 3\%$ for sample 1*u*. Even allowing for these possible errors the data for the two samples do not lie on a common curve, but this is not necessarily unexpected. The residual impurities are probably dif-

ferent in the two cases,⁷ being carbon for sample 1*u* and tungsten for sample 1*a*; this suggests that the anisotropy of the electronic relaxation time τ can be quite different, whereas Kohler's law is derived on the assumption that the anisotropy is independent of the magnitude of τ (or purity).¹⁶

A much more serious problem is the form of the curve. It will be noticed that the slope first increases at relatively low values of rB , reaching a maximum of near 1.90, after which it steadily decreases until it has reached about 1.70 at the highest values of rB (corresponding to a field of about 5.2 T for sample 1*a*). Figure 2 shows a graph of slope against rB , the slope being obtained by differences using neighboring points. The variation at low fields presumably reflects the transition from low- to high-field (or $\omega_c\tau$) conditions, but we anticipate a steadily increasing slope with a limiting value¹⁷ of 2. Typical normal behavior for compensated metals has been observed in W,^{1,18} Cd,² and Pb,¹⁹ where limiting slopes of 1.97⁵, 1.99⁹, and 1.99⁵, respectively, were obtained. The decrease in slope that we observe may be a result of magnetic breakdown causing the appearance of extended orbits; this is in fact a possibility in Mo since the large electron surface at Γ (the jack) and the large hole surface at H are separated^{10,20} only by spin-orbit coupling with a gap of about 0.10 eV. In W the gap is much larger at 0.4 eV,²¹ so similar effects would not be observable in that case. How-

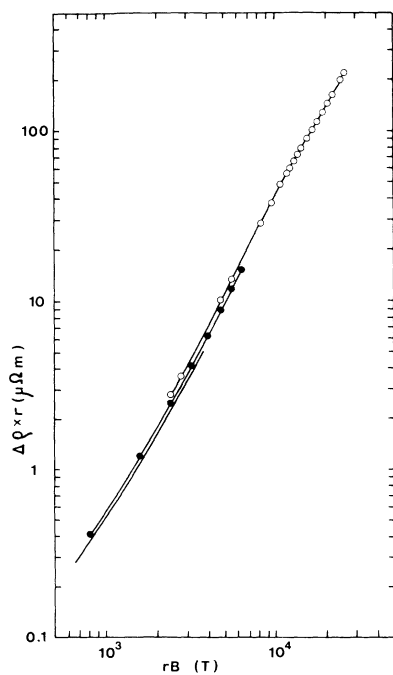


FIG. 1. Change in resistivity $\Delta\rho = \rho_{11}(B) - \rho_{11}(0)$ of Mo as a function of field B . Both axes have been multiplied by the residual resistance ratio r to produce a plot of the Kohler form. \circ , sample 1*a*; \bullet , sample 1*u*; solid line, Fawcett (Ref. 15).

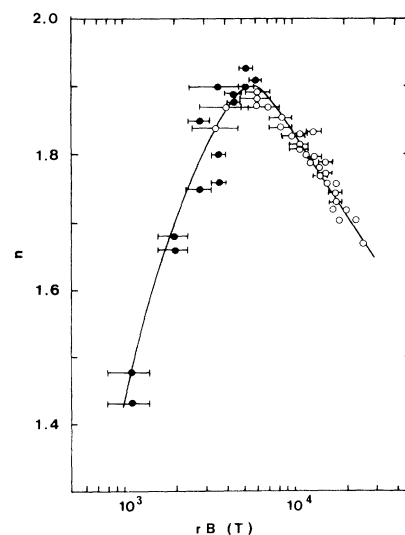


FIG. 2. Slope of Fig. 1 as a function of rB . The slope is obtained by differences between neighboring points on various experimental runs; the error bars represent the spacing of the points used, and where none appear the differences have been taken between points which are closer together than the width of the circles on this graph. \circ , sample 1*a*; \bullet , sample 1*u*.

ever, a problem with this explanation is that the decrease in slope does not occur at a specific B but at a specific value of rB (which is presumably a measure of $\omega_c\tau$). Thus sample 1*u* shows a steady increase in slope to the highest field (~ 3.8 T) to which it was measured, whereas the break in the slope for sample 1*a* appears at about 2 T. Furthermore, Fawcett and Reed²² have looked for breakdown in a Mo sample of $r \sim 830$, with B along [001] up to 8.3 T, and detected no evidence to support such a conjecture.²³ Nevertheless Cabrera and Falicov²⁴ have shown that such breakdown effects can be very purity dependent. They examined two models, both of which could be applicable here, and find that for an impure sample the effects may be much less noticeable. We should point out that ρ_{21} has a magnitude of about 10% of ρ_{11} for sample 1*a*. Thus $\rho_{11} = \sigma_{11}(\sigma_{11}^2 + \sigma_{12}^2)^{-1} \sim \sigma_{11}^{-1}$ should be an excellent approximation in this case, and the discrepancies cannot be attributed to errors due to σ_{12} . (ρ_{21}/ρ_{11} is much higher for sample 1*u*, but the steady decrease in the exponent is not evident for this sample.) Further experimental work on purer samples is certainly warranted.

In the elastic-scattering limit, assuming the lattice conductivity λ_g is zero, the electrical- and thermal-conductivity tensors $\bar{\sigma}$ and $\bar{\lambda}$ should be related by the Weidemann-Franz²⁵ law $\bar{\lambda} = \bar{\sigma}L_0T$, where T is the temperature and L_0 is the Sommerfeld value of the Lorenz number ($\pi^2k^2/3e^2$, k being the Boltzmann constant and e the electronic charge). If thermoelectric terms are ignored, this leads to a similar relation between the resistivity tensors $\bar{\rho} = \bar{\gamma}^e L_0 T$ where the superscript e denotes that we are dealing with the thermal resistivity tensor that would be obtained if λ_g were zero. Phonon scattering is always more effective in influencing thermal compared to electrical transport, so that although ρ_{11} is hardly affected by reducing T below 4.2 K, we expect γ_{11}^e to be changed by a much larger degree. Thus, in general, we will not obtain the Sommerfeld-Lorenz number, but a modified one, say L_1 , defined according to $\rho_{11} = \gamma_{11}^e L_1 T$, where L_1 may be field dependent, though it should saturate²⁶ when $\omega_c\tau \gg 1$. The measured thermal resistivity is modified by the presence of λ_g , and assuming γ_{21}^m is small, one finds²⁸

$$(\gamma_{11}^m)^{-1} = (\gamma_{11}^e)^{-1} + \lambda_g.$$

It is usual to analyze data on γ_{11}^m and ρ_{11} by either plotting $(\gamma_{11}^m)^{-1}$ against $1/B^2$ (e.g., Refs. 1, 2, and 18), or against $(\rho_{11})^{-1}$ (e.g., Ref. 9), and extrapolating to infinite B to obtain λ_g . The following analysis seems to be superior if λ_g is a relatively small fraction of $(\gamma_{11}^m)^{-1}$.

The above equation can be rewritten, making use of L_1 , as

$$\rho_{11}/\gamma_{11}^m T = L_1 + \rho_{11}(\lambda_g/T). \quad (1)$$

If we assume L_1 is independent of B , then a graph of $(\rho_{11}/\gamma_{11}^m T)$ against ρ_{11} will be a straight line of intercept L_1 and slope (λ_g/T) . A selection of such graphs is shown in Fig. 3 (though we have chosen to plot $\rho_{11}/\gamma_{11}^m L_0 T$) and we see that Eq. (1) holds within experimental error. The values of L_1 and λ_g so obtained are shown in Figs. 4 and 5.

At this point a discussion of the possible errors is in order. In the midrange of temperature, say 1.8–3.9 K, the absolute errors arising in γ_{11}^m due to the calibration uncertainties of the carbon resistors should be about 1% at low fields; however these errors may be slightly field dependent and could be (2–3)% at the higher fields, especially at low temperatures (≤ 2.5 K). The errors increase at the ends of the temperature range since small calibration inaccuracies are not so effectively smoothed out by neighboring points. Experience has shown that they rarely exceed 5% with any field-dependent part remaining the same as before. Random errors are about 1% at any temperature, and absolute errors due to the form factor should be less than 5%. In all cases the error in determining the temperature should be negligible. Only the field dependent errors are of importance in determining λ_g ; the heat transported by the lattice is always less than 8% of the total so that a 2% relative uncertainty in γ_{11}^m becomes a 25% uncertainty in λ_g , and this will double at low temperatures where λ_g provides an even smaller contribution. It should be noted that if γ_{11}^m varies approximately as T^{-1} , as is the case here since the electronic scattering is dominated by impurities and λ_g is small, then the use of $\gamma_{11}^m T$ in the analysis, as in Fig. 3, tends to

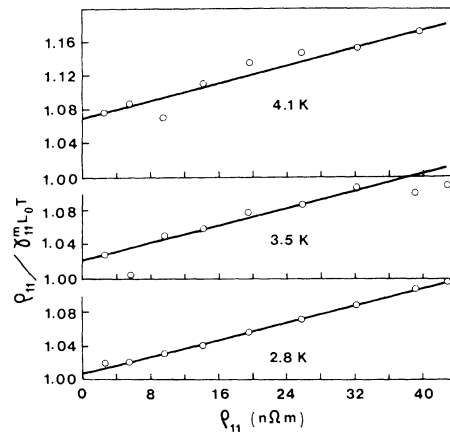


FIG. 3. Typical plots of $\rho_{11}/\gamma_{11}^m L_0 T$ as a function of ρ_{11} at various temperatures. The variation in ρ_{11} is obtained by varying B . The slopes should give $\lambda_g/L_0 T$, and the intercepts at zero ρ_{11} give L_1/L_0 , assuming L_1 is a constant independent of B .

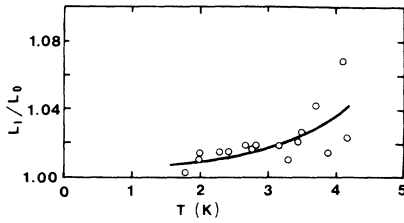


FIG. 4. Variation of L_1 , as obtained from graphs such as those in Fig. 3, as a function of temperature.

eliminate problems with the temperature of the sample varying a little as the field is increased. We see that the value of L_1 is basically determined by the low-field errors and should generally be accurate to about 1% except near the ends of the temperature range. However, the analysis does not enable one to determine if L_1 is field dependent, and indeed it would not be surprising if this were so at the 1% level. Any such variation appears as a magnified error in λ_g . In view of all these problems, we would be surprised if λ_g was more accurate than $\pm 30\%$, and a purer sample would be required to improve on this figure.

The data is consistent with L_1 tending to L_0 at the lowest temperatures and being generally greater than L_0 at higher temperatures. This behavior is similar to that obtained in W and Cd, and is expected on semiquantitative arguments,^{9,18} but detailed calculations do not appear to have been made for any metal. The fact that a limiting value of L_0 is obtained to an accuracy of 1% suggests that the

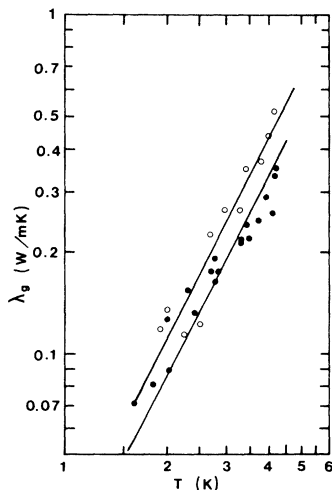


FIG. 5. Lattice thermal conductivity as a function of temperature. The open circles are the results of an analysis of ρ_{21} and γ_{21}^m , the closed circles the results obtained from ρ_{11} and γ_{11}^m . The solid lines are drawn with slope 2, the upper line corresponds to $\lambda_g = 0.027 T^2$ W/mK, and the lower line $0.022 T^2$ W/mK.

thermoelectric coefficients that were ignored in assuming $\bar{\gamma}_{11} = (\bar{\lambda}^m)^{-1}$ must be very small. The results taken with sample 1u could not be usefully analyzed for λ_g , since the latter played an even smaller role in the heat transport, being perhaps 3% of the total at the highest fields and temperature. We found that L_1 was always equal to L_0 within about 2%. In both cases the variation of γ_{11}^e with field is clearly quite consistent with the anomalous variation of ρ_{11} exhibited in Fig. 1.

C. Hall and Righi-Leduc resistivities

The Hall resistivity ρ_{21} of each sample at 4.2 K is shown in Fig. 6 in the form of a Kohler plot. Again the major uncertainty is due to r . Temperature has relatively little effect; for sample 1a ρ_{21} increases (2–3)% on cooling the sample from 4.2 to 1.3 K, and any change for sample 1u is less than 1%. The sign of ρ_{21} is the same as that for W and the magnitude is similar.¹ As in the case of ρ_{11} , a common curve is not obtained and the reasons for this are presumably the same. In view of the fact that ρ_{21} for a compensated metal is a delicate balance between the effects produced by the electrons and holes, it is somewhat surprising that two samples with different impurities need produce such similar results.

The data on sample 1a can be fitted to a variety of expressions involving simple polynomials in B . At 4.2 K and above 1 T, the equation $\rho_{21} = 0.304B + 0.0248B^3$ n Ω m will reproduce the results to about

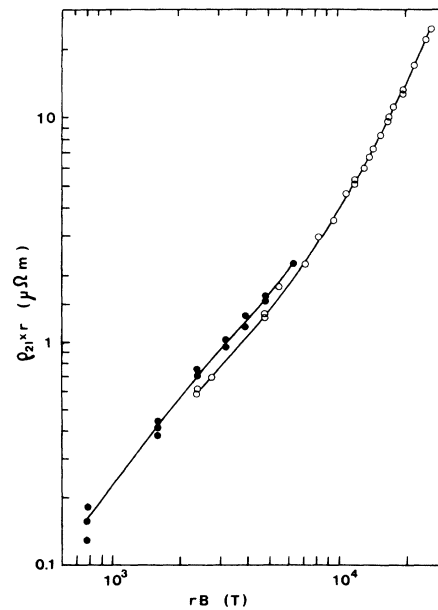


FIG. 6. Hall resistivity ρ_{21} as a function of field B . Both axes have been multiplied by r to produce a Kohler plot. \circ , sample 1a; \bullet , sample 1u.

2%. In contrast to the case of W, an expression of the form $\rho_{21} = a_1 B + a_2 B^2$ provides a very poor fit. It is possible to evaluate $\sigma_{21} = -\rho_{21}/(\rho_{21}^2 + \rho_{11}^2)$, and the expression $\sigma_{21} = -(0.01137/B + 0.0478/B^3)$ ($\text{n}\Omega\text{m}$)⁻¹ reproduces the data on sample 1a extremely accurately with a rms of less than 1% from 0.5 to 5 T, which is about the same level as the relative experimental uncertainty. The absolute error in ρ_{21} should be less than 2%.

If there is really magnetic breakdown in Mo, it may be reflected in the Hall resistivity as well as the transverse resistivity. In general,²⁷ open orbits will produce a transverse even coefficient in σ_{yx} , as well as changing the magnitudes of the odd components. Our sample is oriented with \vec{B} along a cubic axis which, by symmetry, eliminates any transverse even coefficients and without a more detailed understanding of ρ_{21} for compensated models it is impossible to say whether the odd components are partially due to breakdown. We have determined γ_{21}^m as a function of temperature ($1.5 \leq T \leq 4.2$ K) and field ($0.4 \leq B \leq 4.2$ T) and some of the data is shown in Fig. 7 in the form of $\gamma_{21}^m L_0 T$ together with ρ_{21} for comparison. The relative errors in γ_{21} arise from the calibration of the carbon thermometers and will be identical to the case of γ_{11}^m . The thickness of the sample contributes to the absolute error and is known to 1%. The random errors are rather large since γ_{21}^m is very small. The typical change in the carbon resistors due to the Righi-Leduc temperature difference is 0.5% of the total value at the highest fields, and consider-

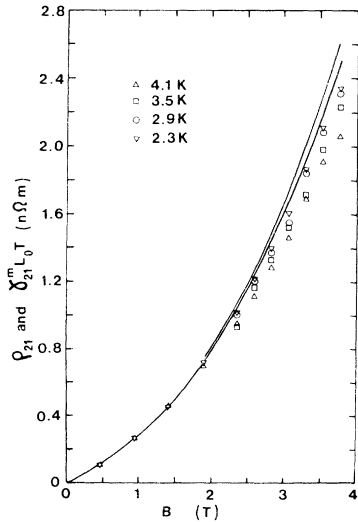


FIG. 7. Measured Righi-Leduc resistivity γ_{21}^m multiplied by $L_0 T$ as a function of field B at various temperatures. The solid lines represent ρ_{21} at 4.2 K (lower) and 1.3 K (upper) for comparison. Some points have been omitted below 2 T for clarity.

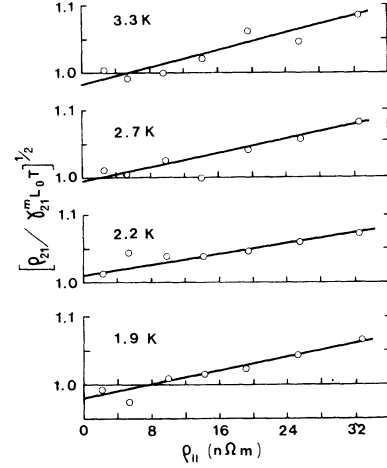


FIG. 8. Typical plots of $(\rho_{21}/\gamma_{21}^m L_0 T)^{1/2}$ as a function of ρ_{11} at various temperatures. The intercepts should yield $(L'_2/L_0)^{1/2}$ and the ratio of slope to intercept $\lambda_g/L_1 T$, assuming L_1 and L'_2 are independent of B .

ably less at low fields.

We have previously shown²⁸ that λ_g modifies γ_{21}^e , i.e., the resistivity that would be appropriate to the electrons in the absence of λ_g , to give the measured value γ_{21}^m , the relation being (assuming $\gamma_{21}^e \lambda_g \ll 1$);

$$\gamma_{21}^m = \gamma_{21}^e (1 + \lambda_g \gamma_{11}^e)^{-2}.$$

If we again assume $\rho_{11} = \gamma_{11}^e L_1 T$ and an analogous²⁹ relation $\rho_{21} = \gamma_{21}^e L'_2 T$, then we obtain

$$\left(\frac{\rho_{21}}{\gamma_{21}^m T}\right)^{1/2} = (L'_2)^{1/2} \left(1 + \frac{\rho_{11} \lambda_g}{L_1 T}\right). \quad (2)$$

Thus a plot of $(\rho_{21}/\gamma_{21}^m L_0 T)^{1/2}$ against ρ_{11} should be a straight line of intercept $(L'_2/L_0)^{1/2}$ and ratio of slope to intercept of $(\lambda_g/L_1 T)$, again assuming L_1 and L'_2 are independent of field. Representative graphs are shown in Fig. 8 and the values of L'_2 and λ_g are shown in Figs. 9 and 5, respectively. The random scatter on L'_2 is high, but all results are consistent with a value tending to L_0 , as T tends to zero, as expected,^{25,26} and a decrease below this value at higher temperatures; this is similar to the case of W but no theory has been developed to ex-

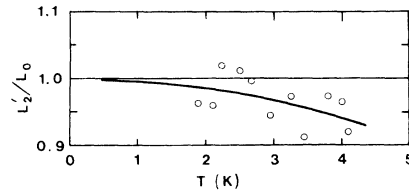


FIG. 9. Variation of L'_2 obtained from graphs such as Fig. 8, with temperature.

plain the temperature dependence.

The values of λ_g derived from the two methods we have presented are not in good agreement but, in view of the small magnitude of λ_g , the discrepancy is not significant. Thus a variation of L'_2 with field to the extent of about 4% is sufficient to produce the difference as is any field-dependent error of similar magnitude in the calibration.

We have previously¹ used a similar (though not identical) analysis for W and found distinctly different values of λ_g by the two methods, the differences being much too large to ascribe to experimental errors or weak variations in Lorenz numbers. In that case we had a much purer sample, with $\omega_c\tau \gg 1$ at all fields, so that the Lorenz numbers should be constant. We suggested^{1,30} that the differences in the case of W arose from the effects of phonon drag by the electronic heat current. Similar arguments should apply in the present case, but the much lower purity of the Mo should lead to a strong decrease in the effect. λ_{21}^m is very small because it is the result of two opposite and almost equal contributions from the electrons and holes. These individual contributions are real in the sense that they correspond to large deviations of the electron and hole distributions from the zero temperature gradient value, and it is as if there were a transverse temperature gradient acting on each of the distributions which is many orders-of-magnitude larger than that which is actually measured, i.e., $\partial T/\partial y$. The ratio of the heat currents carried by the electrons U_e and the phonons U_g in the transverse direction is not λ_{11}^e/λ_g (where $\tilde{\lambda}^e$ is that part of the tensor $\tilde{\lambda}^n$ that is appropriate to the electrons) but is more accurately given by

$$\frac{U_e}{U_g} \sim \frac{\lambda_{21}^e(\partial T/\partial x)}{\lambda_g(\partial T/\partial y)},$$

where we have ignored the contribution $\lambda_{11}^e(\partial T/\partial y)$ in the numerator. The factors²⁶ λ_{21}^e ($\sim ne/B$) and λ_g are essentially purity independent (although λ_g for Mo is about $\frac{2}{3}$ that of W). However $(\partial T/\partial x)/(\partial T/\partial y)$ is very purity dependent and is about 10 for Mo and 200 for W. Now if the drag effect exists at all, then we anticipate that the phonon heat current so produced would be proportional to the deviation from equilibrium of the electronic system (assuming the drag effects are relatively weak and the phonons are not too far from equilibrium), that is, U_e . Presumably the effect will become easier to detect if the normal heat current U_g is small, so we argue that the relative magnitudes of the drag and normal heat currents will contain a factor U_e/U_g . If this is so, then the effect would be 15 times smaller in Mo than W, and would be too small to identify in view of the present uncertainties.

The analysis of γ_{21}^m for sample 1u gave no useful results; γ_{21}^m was always within 5% of ρ_{21}/L_0T at all fields and temperatures.

D. Nernst-Ettingshausen coefficient Q^a

We have shown³ that Q^a should be direct measure of the density-of-states $N(\mu)$ at the Fermi level μ , assuming that phonon drag effects are negligible. More recently,⁴ it has become clear that $N(\mu)$ is the density-of-states with electron-phonon enhancement.

For compensated metals it is found that, to high accuracy,

$$Q^a = \epsilon_{21}^n \rho_{11} = \pi^2 k^2 T N(\mu) \rho_{11} / 3B, \quad (3)$$

where k is the Boltzmann constant and ϵ_{21}^n a component of the thermoelectric tensor $\tilde{\epsilon}^n$. In the event of magnetic breakdown in the xy plane, then σ_{xy} may be modified as we have already pointed out. This will presumably influence ϵ_{xy}^n , since the theory used in deriving Eq. (3) relies on $\epsilon_{xy}^n = -L_0 e T \times (\partial \sigma_{xy} / \partial \epsilon)_\mu$, where e is the (negative) electronic charge and ϵ the electronic energy, the derivative being evaluated at the Fermi energy μ . However we recall that σ_{xy} is the resultant of two large terms of opposite sign but of almost equal magnitude (arising from the holes σ_{xy}^h and electron σ_{xy}^e). In taking the energy derivative these terms become additive giving a large ϵ_{xy}^n . Any contribution to σ_{xy} due to breakdown must be relatively small compared to either σ_{xy}^h or σ_{xy}^e , since the measured σ_{xy} is itself small. Assuming the number of electrons per atom is about unity for Mo, then $\sigma_{xy}^e \sim ne/B \sim 10^{10}/B$ (Ωm)⁻¹, which should be compared with the experimental value of $\sigma_{xy} \sim 4 \times 10^6$ (Ωm)⁻¹ at a field of 4 T. Thus the neglect of the small number of electrons participating in breakdown should cause no significant error in the evaluation of ϵ_{xy}^n .

The transverse voltages were small, being perhaps 200 nV in the best case of high field and high temperature. The potential leads were manganin which has a thermopower³¹ of roughly 0.1T $\mu\text{V}/\text{K}$ in the temperature range of interest, T being the temperature; the transverse Righi-Leduc temperature differences were very small, being less than 5 mK, so that correction due to the thermoelectric power of the leads were also very small, and typically 1% of the Nernst-Ettingshausen voltage. It was necessary to use relatively large heater powers to produce the largest possible signals, and this tended to produce changes in the absolute temperature of perhaps 0.1–0.15 K, as B was increased. Assuming Q^a is approximately linear in T , then an analysis in terms of Q^a/T will suppress the effect of these variations, and this was, in fact, the approach taken. Figure 10 shows a typical set

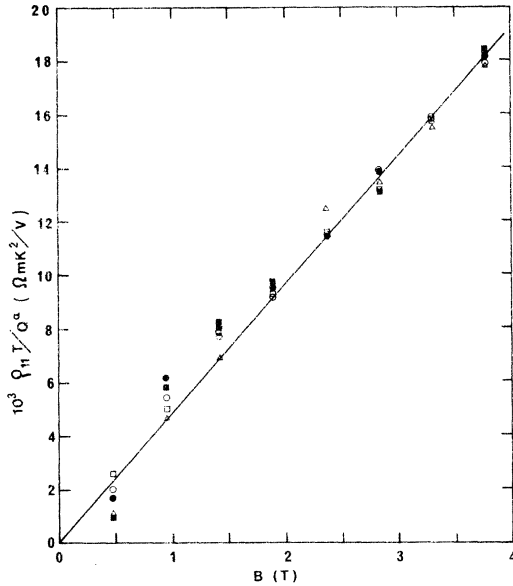


FIG. 10. Quantity $\rho_{11}T/Q^a$, which is equivalent to T/ϵ_{21}^n , as a function of field for one particular experimental run. The symbols represent different temperatures: \bullet , 4.21; \circ , 3.70; \triangle , 3.20; \blacksquare , 2.65; \square , 2.00 K.

of data for $\rho_{11}T/Q^a (= T/\epsilon_{21}^n)$ as a function of B , and it is evident that within experimental error, a single line reproduces all the results. This confirms that ϵ_{21}^n varies linearly in T as would be expected if phonon drag effects are small. It is of interest to note that Q^a is not linear in B , since ρ_{11} does not vary as B^2 , but that ϵ_{21}^n does vary accurately as B^{-1} . If one uses the mean values of $\rho_{11}T/Q^a$ over various temperatures at a given field for different sets of experimental data, then Fig. 11 results. Although the data seems to lie consistently above the line at low B , one should bear in mind that the result in Eq. (3) is that appropriate to very high fields ($\omega_c\tau \gg 1$ for all orbits) and need not hold accurately at low fields. Furthermore, the experimental uncertainties rapidly increase at lower fields. For both of these reasons, emphasis must be placed on the data at higher fields. The slope of this graph can be used to evaluate $\frac{1}{3}\pi^2k^2N(\mu)$, and gives $207.5 \text{ J m}^{-3} \text{ K}^{-1}$, with an error of probably less than 5% (this estimate being based on our previous experience with Cd)³. The same quantity can be evaluated from specific-heat data¹³ which yields $196 \text{ J m}^{-3} \text{ K}^{-1}$. If the transport result had not included the electron-phonon enhancement factor λ (which has been estimated as 0.41 experimentally and 0.22 theoretically³²) then we would have expected a value for the above quantity of perhaps $140\text{--}160 \text{ J m}^{-3} \text{ K}^{-1}$. Clearly the experimental data is in much better agreement with the enhanced val-

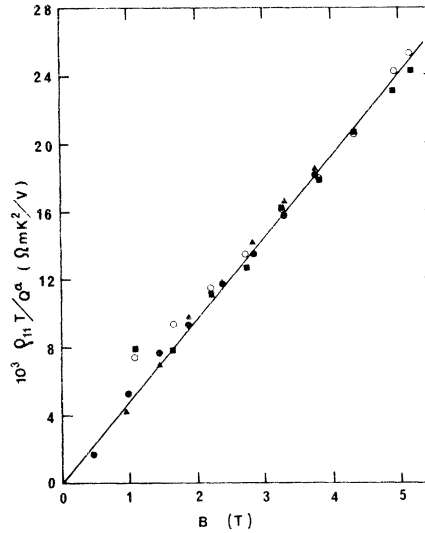


FIG. 11. Mean values of $\rho_{11}T/Q^a$ as a function of B , the averages being taken over for any particular run at fixed field and different temperatures. The various symbols represent different runs.

ue. Our previous results³ on Cd are not inconsistent with the enhanced value of $N(\mu)$, but these on W are still not understood. Little data was taken on Q^a for sample 1μ since the much lower effective purity meant that the transverse voltages were very small and the larger pieces of Fermi surface only marginally satisfy the high field condition. The results suggested that $\rho_{11}T/Q^a$ was larger for this sample by roughly 25%, possibly indicating a dependence of this quantity on purity. However the results were too few and too inaccurate to be reliable.

IV. CONCLUSIONS

The work reported in this paper has attempted to provide a complete set of results (with the exception of the thermoelectric coefficient ϵ_{11}) on the various transport coefficients of a Mo single crystal at temperatures of 1.5–4.2 K with the magnetic field perpendicular to the current. Generally speaking, all the data is consistent with that which would be expected for a normal compensated metal but several aspects of the work deserve further study. The ordinary transverse resistivity ρ_{11} does not show a limiting behavior of B^2 , and an investigation using purer samples would be of interest. There are no first-principles calculations for the Hall resistivity ρ_{21} of any compensated metal; the similarities between W and Mo indicate the observed behavior is intrinsic to the electron (and possibly phonon) spectra, and with the available

detailed band structure³² should be amenable to calculation. The corresponding thermomagnetic coefficients behave generally as expected, but in particular there is no available theory for L'_2 . The estimates of the lattice conductivity obtained by

the two methods outlined are not in perfect agreement, but are within the expected errors incurred in the experiments and analysis. Finally, the Nernst-Ettingshausen coefficient is in agreement with expectation.

*Work supported by NRC of Canada.

¹R. Fletcher, *Philos. Mag.* **32**, 565 (1975).

²R. Fletcher, *J. Low Temp. Phys.* **22**, 39 (1976).

³R. J. Douglas and R. Fletcher, *Philos. Mag.* **32**, 73 (1975).

⁴J. L. Opsal, B. J. Thaler, and J. Bass, *Phys. Rev. Lett.* **36**, 1211 (1976).

⁵The Mo crystal was obtained from Koch-Light Labs. Ltd., Colnbrook, Bucks, England, and was listed as 99.99% in purity.

⁶The silver paint and plastic cement was manufactured by G. C. Electronics, Rockford, Ill.

⁷D. J. Capp, H. W. Evans, and B. L. Eyre, *J. Less-Common Metals* **40**, 9 (1975).

⁸C. G. Grenier, J. M. Reynolds, and J. R. Sybert, *Phys. Rev.* **132**, 58 (1963).

⁹J. R. Long, *Phys. Rev. B* **3**, 1197 (1971); **3**, 2476 (1971).

¹⁰T. L. Loucks, *Phys. Rev.* **139**, A1181 (1965).

¹¹V. V. Boiko, V. A. Gasparov, and I. G. Gverdtsiteli, *Zh. Eksp. Teor. Fiz.* **56**, 489 (1969) [*Sov. Phys.-JETP* **29**, 267 (1969)].

¹²G. T. Meaden, *The Electrical Resistance of Metals* (Plenum, New York, 1965).

¹³A. J. Arko and F. M. Mueller, *Phys. Kondens. Mater.* **19**, 231 (1975); *Phys. Rev. Lett.* **29**, 1515 (1972).

¹⁴N. E. Phillips, *C. R. C. Crit. Rev. Solid State Sci.* **2**, 467 (1971).

¹⁵E. Fawcett, *Phys. Rev.* **128**, 154 (1962).

¹⁶R. G. Chambers, *Proc. R. Soc. Lond. A* **238**, 344 (1956).

¹⁷I. M. Lifshitz, M. Ia. Azbel', and M. I. Kaganov, *Zh. Eksp. Teor. Fiz.* **31**, 63 (1956) [*Sov. Phys.-JETP* **4**, 41 (1957)].

¹⁸D. K. Wagner, *Phys. Rev. B* **5**, 336 (1972).

¹⁹The measurements on Pb have been carried out by M. R. Stinson and have not been published.

²⁰R. J. Iverson and L. Hodges, *Phys. Rev. B* **8**, 1429 (1973).

²¹L. F. Mattheis, *Phys. Rev.* **139**, A1893 (1965).

²²E. Fawcett and W. A. Reed, *Phys. Rev.* **134**, A723 (1964).

²³N. E. Alekseevskii, V. A. Egorov, G. E. Karstens, and B. N. Kazak, *Zh. Eksp. Teor. Fiz.* **43**, 731 (1962) [*Sov. Phys.-JETP* **16**, 519 (1963)]. This reference gives magnetoresistance results on two Mo single crystals of rather low purity. Although some of the data is taken up to fields of 18 T, the orientation of the crystals was not appropriate to observing breakdown orbits.

²⁴G. G. Cabrera and L. M. Falicov, *Phys. Rev. B* **10**, 4803 (1974).

²⁵M. Kohler, *Ann. Phys. (Leipz.)* **6**, 18 (1949). See also Ref. 26.

²⁶M. Ia. Azbel', M. I. Kaganov, and I. M. Lifshitz, *Zh. Eksp. Teor. Fiz.* **32**, 1188 (1957) [*Sov. Phys.-JETP* **5**, 967 (1957)].

²⁷C. M. Hurd, *The Hall Effect in Metals and Alloys* (Plenum, New York, 1972).

²⁸R. Fletcher, *J. Phys. F* **4**, 1155 (1974).

²⁹We use L'_2 rather than L_2 to keep the notation consistent with that used in Refs. 1, 8, 9.

³⁰R. Fletcher, *Proceedings of the Fourteenth International Conference on Thermal Conductivity, Storrs, Connecticut, 1975*, edited by P. G. Klemens and T. K. Chu (Plenum, New York, 1976), p. 121.

³¹G. A. Slack, *Phys. Rev.* **122**, 1454 (1961).

³²D. D. Koelling, F. M. Mueller, A. J. Arko, and J. B. Ketterson, *Phys. Rev. B* **10**, 4889 (1974).